Pionic Fusion of Heavy Ions

D. Horn, G. C. Ball, D. R. Bowman, W. G. Davies, D. Fox, A. Galindo-Uribarri, A. C. Hayes, and G. Savard

AECL, Chalk River Laboratories, Chalk River, Ontario, Canada K0J 1J0

L. Beaulieu, Y. Larochelle, and C. St-Pierre

Laboratoire de Physique Nucléaire, Département de Physique, Université Laval, Ste-Foy, Québec, Canada G1K 7P4

We report the first experimental observation of the pionic fusion of two heavy ions. The ^{12}C(^{12}C, ^{24}Mg)π^0 and ^{12}C(^{12}C, ^{24}Na)π^+ cross sections have been measured to be 208 ± 38 and 182 ± 84 pb, respectively, at $E_{cm} = 137$ MeV. This cross section for heavy-ion pion production, at an energy just 6 MeV above the absolute energy-conservation limit, constrains possible production mechanisms to incorporate the kinetic energy of the entire projectile-target system as well as the binding energy gained in fusion.   [S0031-9007(96)01190-8]

Pionic fusion, the creation of a pion in a reaction fusing two nuclei, requires the concentration of the kinetic and potential (binding) energy of the projectile-target system into a few degrees of freedom, namely, the rest mass and emission energy of a pion, with possible, discrete emission energies determined by the limited number of available final states of the fusion product. The phenomenon has previously been observed for the ^{3}He(^{3}He, π^+)^{6}Li reaction [1] and subsequently for ^{3}He-induced reactions with heavier targets [2,3]. Until now, it has been a matter of conjecture whether reactions between two heavy ions would manifest the degree of coherence necessary for pionic fusion. By contrast, the inclusive creation of pions in heavy-ion reactions at "subthreshold" energy (i.e., at an energy per nucleon below the nucleon-nucleon pion production threshold) has been studied extensively (see Refs. [4] and [5] for reviews). However, low experimental efficiencies for pion detection make measurements of subnanobarn cross sections difficult; as a result experiments have been limited to center-of-mass energies 100 MeV or more above absolute threshold [6,7]. Even at those energies, mechanisms based upon on-shell nucleon-nucleon collisions [5] could not account for the observed pion production cross sections, and a number of cooperative or coherent mechanisms were proposed, including "pionic bremsstrahlung" [8] and statistical compound nucleus emission of pions [9,10]. To date, the application of fully quantum-mechanical models for pion production in fusion reactions has been limited to cases in which the projectile is a proton [11]. Motivated by the successful descriptions [12] of the $p + p \rightarrow d + \pi^+$ reaction, these models usually involve three basic ingredients: a primary nucleon-nucleon pion production mechanism, an amplitude for rescattering this virtual pion on-shell, and a nuclear structure form factor describing the required spectroscopic amplitudes and the momentum distributions of the wave functions. An extension of these microscopic models to the present ^{12}C + ^{12}C reaction, which has projectile-target symmetry and an isoscalar entrance channel, necessarily requires

at least two nucleons in the pion production amplitude. Then, in the simplest picture, one of the ^{12}C nuclei may be excited to a $T = 1$ state producing a virtual pion, and the pion then rescattered on-shell from the second ^{12}C. The pseudoscalar nature of the pion production vertex means that only unnatural-parity $T = 1$ states of ^{12}C are involved. Thus the cross section depends sensitively on the nuclear structure spectroscopic amplitudes for expressing the final states of the mass-24 product in terms of the coupling of $T = 1$ one-particle-one-hole unnatural-parity states of ^{12}C to the ^{12}C ground state.

This Letter reports the first observation of heavy-ion pionic fusion. The very low center-of-mass energy relative to threshold requires a coherent production process. The cross sections may be linked with the existing systematics of inclusive ^{12}C(^{12}C, π^0) measurements at higher energies [4,5]. The pionic fusion channel, in particular, provides a reference point for calculations of various proposed statistical or thermal production processes, since the initial conditions (compound nucleus mass, charge, and excitation energy) are determined by the fusion process. In addition, the present restriction to an isoscalar entrance channel provides a constraint on existing microscopic models, which may lead to an understanding of the dominant reaction mechanism at "subthreshold" energies.

In order to measure cross sections in the subnanobarn range, where π^0-decay studies are hampered by background and efficiency considerations, and charged-pion detection is limited by spectrometer solid angle, we have chosen to detect the mass-24 fusion products of the ^{12}C(^{12}C, ^{24}Mg)π^0 and ^{12}C(^{12}C, ^{24}Na)π^+ reactions, rather than the pions themselves. Any ^{24}Mg compound nucleus formed without emitting a high-energy quantum, such as a pion or a bremsstrahlung photon, should decay by nucleon or cluster emission, giving a lower mass. High-energy photon emission can be excluded kinematically by the large momentum it transfers to the recoil. This makes mass-24 recoils, moving with the approximate center-of-mass velocity of the reaction, a reliable signature of pionic

fusion. At $E_{cm} = 137$ MeV, the total energy available is only about 6 MeV above that necessary to produce a positive or neutral pion and the corresponding $A = 24$ isobar in its lowest $T = 1$ state; the π^- channel is energetically forbidden.

A ^{12}C beam of $E_{lab} = 274.2 \pm 1.2$ MeV from Chalk River's TASCC facility was incident on a thick, isotopically separated ^{12}C target, 826 μg/cm^2 in areal density. The target was prepared with precautions to minimize contamination, baked in a vacuum oven, and stored and transferred in an inert atmosphere. With the assumption of a maximum-energy 6 MeV pion emitted transversely and with allowance for multiple scattering in the target, the ^{24}Na and ^{24}Mg products recoil within 1° of the beam axis. We therefore aligned the Chalk River Q3D spectrometer [13] at $\theta_{lab} = 0°$ and collimated its entrance with a circular aperture of 1 msr solid angle, corresponding to a cone of 1° half angle. The main carbon beam was stopped and current integrated on a beam block positioned inside the spectrometer's magnet box; additional cleanup of scattered beam was provided by a scraper paddle further into the spectrometer. Ions with the appropriate momentum-to-charge ratio were deflected to the spectrometer's focal plane and registered in a heavy-ion counter [14]. The first layer of the detector was an avalanche counter operating at 10 Torr and providing timing and position information. The avalanche counter was built in two halves, with a dead region between them reducing the total detector efficiency to 94%. This layer was followed by a second gas volume at about 200 Torr, which contained proportional wires for determination of energy loss and position, an ionization chamber volume to measure residual energy, and finally an anticoincidence region to reject events arising from ions (mainly scattered or degraded beam particles), failing to stop in the E detector. Events electronically imitating mass-24 recoil signals, such as several ions reaching the counter at nearly the same time, were largely eliminated by timing, pileup rejection, and anticoincidence requirements. A more severe problem was presented by genuine ^{24}Na and ^{24}Mg ions formed in reactions with heavier-than-carbon target contaminants (chiefly oxygen); their presence necessitated a detailed examination of background yields. The momentum calibration was obtained from the position signals produced with a 138 MeV ^{24}Mg beam for various spectrometer magnetic fields. The charge-state distributions for 120 to 150 MeV ^{24}Mg ions exiting a carbon target were explicitly measured (more than half were fully stripped) and the results extrapolated for sodium. Since the momentum acceptance of the focal plane detector spanned about 4.7%, four spectrometer field settings were needed to cover the momentum range in the vicinity of the beam momentum for mass-24 ions of charge 11 and 12, and data from 7500 μC of ^{12}C^{6+} beam ions were collected at each setting.

The Galilean-invariant yields for ^{24}Na and ^{24}Mg are shown as a function of velocity in the upper and lower panels, respectively, of Fig. 1. The spectra are not back-
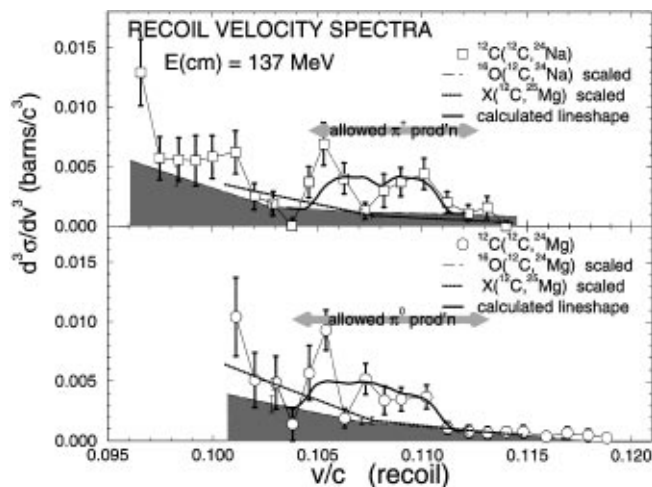

FIG. 1. Galilean-invariant cross sections as a function of recoil velocity, obtained from the thick-target data, for the reactions ^{12}C(^{12}C, ^{24}Na) (top panel) and ^{12}C(^{12}C, ^{24}Mg) (bottom panel) at $E_{cm} = 137$ MeV. For consistency, data are binned by position on the spectrometer focal plane, rather than by analyzed velocity. The double-headed arrows indicate the possible range of recoil velocity distributions from the π^+ (top) and π^0 (bottom) pionic fusion reactions. The shaded regions represent the measured $A = 24$ yields from the ^{12}C + ^{16}O reaction, scaled to represent the background due to oxygen contamination of the target; the dotted line is an alternative background determination based on ^{25}Mg yields. The solid curves represent one possible calculated line shape, illustrating the expected width. See text for details and line-shape calculation.

ground subtracted but are corrected for dead time and detector efficiency. The expected widths of the velocity distributions, the calibration uncertainties, resolution effects, energy-loss straggling in the target, and the possible range of beam energies combine to determine the "allowed" velocity ranges for pionic fusion residues (indicated by the double-ended arrows), over which the yield is integrated to obtain the gross cross sections listed in the first column of Table I.

Note the nonzero yields outside of the "allowed" velocity ranges, especially the rise in yield toward velocities well below the center-of-mass velocity of the ^{12}C-^{12}C system. Such an increase at low velocity would be characteristic of evaporation residues from fusion reactions with target contaminants heavier than carbon. Analysis of the target composition by the ERD technique [15] revealed the presence of oxygen contamination at the 1% level and a smaller amount of aluminum contamination. To obtain the spectral shape of the background due to oxygen, the major contaminant, within the allowed velocity region, we have measured the ^{16}O(^{12}C, ^{24}Na) and ^{16}O(^{12}C, ^{24}Mg) yields from a 150 μg/cm^2 MoO$_2$ target. We then obtained the ^{24}Na and ^{24}Mg background levels by normalizing the ^{23}Na and ^{23}Mg yields from the oxygen reaction to those from the carbon target, where the main source of mass-23 ions is contamination. (Single-nucleon emission from the ^{12}C + ^{12}C reaction would cause the $A = 23$ residue to recoil outside the region of velocity space allowed for pionic fusion

TABLE I. Gross, background, and background-subtracted cross sections for the $^{12}C(^{12}C, ^{24}Mg)$ and $^{12}C(^{12}C, ^{24}Na)$ reactions with thick (826 $\mu g/cm^2$) and thin (486 $\mu g/cm^2$) targets at $E_{cm} = 137$ MeV in the region of "allowed" recoil velocities for pionic fusion. Also listed is the subthreshold ($E_{cm} = 130$ MeV) thin-target measurement for the $^{12}C(^{12}C, ^{24}Mg)$ reaction.

Measurement	Counts	σ_{gross} (pb)	σ_{bkgd} (pb)	σ_{net} (pb)
^{24}Mg (thick)	98	397(40)	166(25)	231(47)
^{24}Na (thick)	68	353(43)	126(22)	227(48)
^{24}Mg (thin)	58	329(43)	163(46)	166(63)
^{24}Na (thin)	7	159(82)	136(38)	23(90)
^{24}Mg (subthreshold)	14	279(90)	220(62)	59(109)

residues.) The resulting background levels are indicated by shading in Fig. 1. Their shape is that of the oxygen contaminant products, but their yield, from the normalization to mass-23 carbon-target products, represents the *total* contaminant product cross section for ^{24}Na and ^{24}Mg. The background cross sections, integrated over the same velocity range as the carbon-target data, are listed in the table and used in the determination of the net yields for the pionic fusion process. The background cross sections obtained are consistent with those interpolated from the mass-24 yield on each side of the "allowed" region.

With decreasing velocities, the carbon-target data apparently rise even more steeply than the oxygen-target background measurement. Heavier contaminants, such as aluminum, produce mass-24 residues more readily than oxygen does, and would give such a low-velocity rise, but these products have little impact in the velocity range of pionic fusion residues, since their distributions are peaked at even lower velocities than those from oxygen contamination. We have made a third independent background assessment based on the shape of the ^{25}Mg spectrum, which samples all the heavier-than-carbon contaminants on our carbon target. When normalized to the mass-24 yields at $v_{recoil} = 0.103c$, below the allowed velocity range for pionic fusion residues, the backgrounds obtained by this method (dotted lines in the figure) agree with the ^{24}Na and ^{24}Mg oxygen background measurements listed in the table to within 30 pb. The consistency between the three independent background evaluations demonstrates that the contaminant effects are quantitatively understood and confirms the reliability of the background-subtracted cross sections.

The shape of the recoil velocity distribution carries information about the kinematics of the emitted pion. The well-known forward-backward peaking observed in $^{12}C(^{12}C, \pi^0)$ reactions at higher energies [16] should combine with the phase-space preference for higher emission energies to produce a depletion in recoil yield at the center-of-mass velocity. The primary distribution of recoil velocities resulting from full-energy pion emission (i.e., to the lowest $T = 1$ state) and a cosine-squared pion angular distribution as measured in the $^3He(^3He, \pi^+)^6Li$ reaction [1] is plotted in the top panel of Fig. 2. The line shape expected after energy loss for ^{24}Mg recoils produced over an 826 $\mu g/cm^2$ range of target thickness and smeared by straggling, resolution effects, and final-state gamma-ray

emission is drawn as a heavy dashed line; for this target thickness the depleted velocity region is filled in. The line shape for a thinner target (solid line) retains its central valley.

To search experimentally for the kinematic signature of the pionic fusion process, additional measurements were made with thinner, 486 $\mu g/cm^2$ targets. Their sum is shown in the lower half of Fig. 2, illustrating the characteristic depletion in ^{24}Mg yield at the center-of-mass velocity. The cross section for the thin-target measurements are listed in Table I. The ^{24}Mg results are in agreement with thick-target data, but the ^{24}Na yields, for which only one low-statistics experiment is available, are inconclusive. The net cross section expected on the basis of the thick-target data (227 pb) should have a total uncertainty of ±198 pb, indicating that our actual experimental result of 23 ± 90 pb has little statistical significance. The result does, however, lower the weighted average cross section by some 20% relative to the thick-target data alone, and should therefore not be ignored in the averaging.

The radiative capture reaction (fusion followed by emission of gamma rays only) could also contribute ^{24}Mg ions at these velocities. It was therefore decided
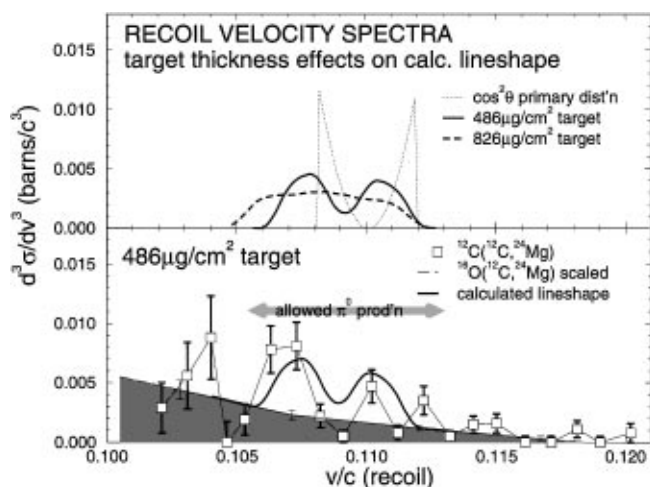

FIG. 2. Top panel: Velocity line shape expected for pionic fusion residues assuming a $\cos^2 \theta$ pion angular distribution (dotted line). Broadening effects are shown for target thicknesses of 486 $\mu g/cm^2$ (solid line) and 826 $\mu g/cm^2$ (dashed line). Bottom panel: As Fig. 1, but for $^{12}C(^{12}C, ^{24}Mg)$ thin-target data.

to use the same target to measure the ^{24}Mg yield at $E_{cm} = 130$ MeV, which is just below the absolute threshold for the ^{12}C(^{12}C, ^{24}Mg[$T = 1$])π^0 reaction. At this energy, the radiative capture cross section should be essentially unchanged, but pionic fusion is forbidden. The background-subtracted cross section is 59 ± 109 pb, which is consistent with zero (within half a standard deviation) and inconsistent (by 1.4 standard deviations) with the average above-threshold cross section. With this level of experimental uncertainty, the radiative capture process cannot be conclusively eliminated on the basis of our data; however, a number of additional factors argue against it, such as the shape of the thin-target velocity distribution, the kinematic exclusion of single-photon emission, and the relative improbability of multiple high-energy photon emission (statistical-model calculations [17] are 3 orders of magnitude lower than the measured cross sections). Furthermore, radiative capture is not a possible source of ^{24}Na ions.

To assess the significance of the cross sections in terms of overall heavy-ion pion production, it is necessary to know what other pionic exit channels are open. For the π^+ channel, the only final states allowed by energy conservation involve particle-stable levels in ^{24}Na. The ^{12}C(^{12}C, ^{24}Na)π^+ yield of 182 ± 84 pb, averaged from the thick-target and thin-target measurements, therefore represents the entire π^+ cross section. (Because of the disparity between the measurements, we follow the common practice of inflating the uncertainty on the mean by a factor of $\sqrt{\chi^2/N_F}$.) The π^0 channel has a larger energy range for allowed final states in ^{24}Mg, but the upper half of this range is particle unbound. A more detailed accounting of the specific $T = 1$ levels available, their particle decay widths, and phase-space factors indicates that about half the ^{24}Mg residues produced in the π^0 reactions survive. This, together with the expected isospin relationship for the π^+ and π^0 channels and the effect of the Coulomb barrier on π^+ decay, should result in a mass-24 residue yield that is comparable for the two pion channels. The average measured ^{12}C(^{12}C, ^{24}Mg) cross section of 208 ± 38 pb is therefore consistent with this estimate. Extrapolation of the inclusive π^0 production systematics [4,5] to lower energy should be reliable to within a factor of 2 or 3 and gives 500 pb for our reaction. The measured cross section, representing about half the inclusive yield, is in agreement with these systematics. The impact of the experimental results on some of the currently available models is illustrated below.

(i) Standard heavy-ion particle-production models (e.g., Ref. [5]), based on incoherent summation of on-shell nucleon-nucleon collisions, are appropriate at higher energies, but severely underpredict our near-threshold results.

(ii) The pionic bremsstrahlung model [8] requires $E_{cm} \geq m_\pi c^2 + E_{Coul}$, since the relatively gentle deceleration from the Coulomb barrier (about 10 MeV for ^{12}C + ^{12}C) should not contribute to pion production. With $E_{cm} \approx m_\pi c^2$, the present pionic fusion reactions would not have sufficient kinetic energy to produce pionic bremsstrahlung after Coulomb deceleration.

(iii) A test of various thermal and statistical models [9,10] should also be possible with pionic fusion data. For inclusive pion production, the thermal approach depends on models of reaction dynamics to define the size and excitation of the emitting volume; for pionic fusion, these quantities are known. Furthermore, with a two-body exit channel, the pion emission energy is defined by the known low-lying $T = 1$ states in the final nucleus.

(iv) Microscopic models [11,18] require the $T = 0$ target or projectile to be excited to a $T = 1$ particle-hole state; experimental observation of pions in the present reaction necessitate at least two nucleons in the pion production amplitude. In addition, pionic fusion of two heavy ions pushes the models further off shell than do proton-induced reactions.

In summary, the ^{12}C(^{12}C, ^{24}Mg)π^0 and ^{12}C(^{12}C, ^{24}Na)π^+ cross sections have been measured to be 208 ± 38 and 182 ± 84 pb, respectively, at $E_{cm} = 137$ MeV. This constitutes the first observation of the pionic fusion of two heavy ions. It also provides a low-energy measurement, just 6 MeV above absolute threshold, for the extensive heavy-ion π^0 production systematics, which had only been studied previously at energies more than 100 MeV above threshold. Our measurement of appreciable yields so near threshold will require models to incorporate coherent mechanisms for pion production.

[1] Y. Le Bornec et al., Phys. Rev. Lett. **47**, 1870 (1981).
[2] L. Bimbot et al., Phys. Rev. C **30**, 739 (1984).
[3] W. Schott et al., Phys. Rev. C **34**, 1406 (1986).
[4] Peter Braun-Munzinger and Johanna Stachel, Annu. Rev. Nucl. Part. Sci. **37**, 97 (1987).
[5] W. Cassing et al., Phys. Rep. **188**, 363 (1990).
[6] G. R. Young et al., Phys. Rev. C **33**, 742 (1986).
[7] M. Waters et al., Nucl. Phys. **A564**, 595 (1993).
[8] D. Vasak et al., Nucl. Phys. **A428**, 291c (1984).
[9] M. Prakash et al., Phys. Rev. C **33**, 937 (1986).
[10] L. Potvin et al., Phys. Rev. C **38**, 2964 (1988).
[11] Harold W. Fearing, in *Pion Production and Absorption in Nuclei*, edited by Robert D. Bent, AIP Conf. Proc. No. 79 (AIP, New York, 1982).
[12] B. Goplen, W. R. Gibbs, and E. L. Lomon, Phys. Rev. Lett. **32**, 1012 (1982).
[13] J. C. D. Milton et al., Atomic Energy of Canada Internal Report No. AECL-3563, 1970.
[14] G. C. Ball et al., Nucl. Phys. **A325**, 305 (1979).
[15] J. S. Forster et al., Report No. TASCC-P-95-28; Nucl. Instrum. Methods Phys. Res., Sect. B (to be published).
[16] E. Grosse, Nucl. Phys. **A447**, 611c (1985).
[17] M. Chadwick (private communication).
[18] W. R. Gibbs, in *Pion Production and Absorption in Nuclei* (Ref. [11]).